Gut Microbiota Mediates Oolong Tea Polyphenols Alleviation of Circadian Rhythm Disturbance

Ruonan Yan
Ningbo University
Chi-Tang Ho
Rutgers University New Brunswick
Yanan Liu
Ningbo University
Ruilin Zhang
Ningbo University
Zufang Wu
Ningbo University
Peifang Weng
Ningbo University
Xin Zhang (zhangxin@nbu.edu.cn)
Ningbo University https://orcid.org/0000-0002-5795-9197

Research

Keywords: gut microbiota, circadian rhythm, oolong tea polyphenols, single-cell sequencing, metabolism

Posted Date: August 10th, 2021

DOI: https://doi.org/10.21203/rs.3.rs-769896/v1

Abstract

Background

Tea polyphenols can be digested in the intestinal tract so as to promote the growth of helpful gut microbiota, and through the production of catechin, tryptophan, acetic acid and other active substances which involved in the modulation of circadian rhythms mechanism to improve the circadian rhythm disorders and neurological weakness, while its specific mechanism is still unclear. The interaction between host circadian rhythm and gut microbes through the gut-brain axis (GBA) provides new clues for tea polyphenols to improve host health. Our present research mainly investigated the metabolites of the gut microbiota and the heterogeneous expression of circadian rhythm genes in the liver and hypothalamic, and then revealed the modulatory role of oolong tea polyphenols (OTP) of circadian rhythm disorder *via* the GBA. We used 16S rDNA and untargeted metabolomics sequencing techniques to analyze the effects of OTP on intestinal flora diversity and abundance of specific flora in mice with diurnal disorders, and to screen out marker metabolites which may be involved in circadian rhythm regulation. Transcriptomics and 10X single-cell sequencing were used to evaluate the effects of OTP on circadian rhythm genes in liver and hypothalamus and hypothalamus cell types in mice with diurnal disorders. The Y maze and Morris water maze experiments were investigated the effects of OTP on long-term and short-term memory impairment.

Results

By establishing a circadian rhythm disorder mouse model, our experimental results showed that OTP improved the structural disorder of the intestinal microbiota caused by continuous darkness, especially significantly decreased the ratio of Firmicutes/Bacteroidetes (F/B), thereby modulating the production of metabolites related to pyruvate metabolism, glycolysis/gluconeogenesis, and tryptophan metabolism to alleviate the steady-state imbalance caused by circadian rhythm disorders. In addition, OTP can significantly ameliorate the rhythm oscillation disorder of specific gut microbes and liver clock genes induced by continuous darkness, and made dysrhythmic mice perform well in cognitive behavior tests. Simultaneously, OTP intervention increased the number of rhythmic expression genes in the liver which in the CD group has 156, while in the OTP group has 208. Transplanting fecal microbiota from the OTP group into germ-free mice exhibited that OTP significantly increased the number of hypothalamus cell clusters, up-regulated the number of astrocytes and fibroblasts, and enhanced the expression of circadian rhythm genes *Cry2*, *Per3*, *Bhlhe41*, *Nr1d1*, *Nr1d2*, *Dbp*, and *Rorb* in hypothalamic cells.

Conclusions

Our results confirmed that OTP reduced the F/B ratio, made the daily oscillation of the intestinal microbiota tended to be regular, actively improve the intestinal microecological status, the content of important metabolite closely associated with circadian rhythm such as Tryptophan, Glutamine, 2-indolecarboxylic acid and some others has been significantly increased, the poor expression of clock genes (such as *Cry2, Per3, Bhlhe41, Nr1d1, Nr1d2, Dbp* and *Rorb*) in liver and hypothalamus cells has

been improved. These results indicated that OTP can significantly improve the metabolic imbalance and cognitive impairment caused by the circadian rhythm disorder, maintain the host's homeostasis, which with potential prebiotic functional characteristics to positively contribute to host health.

Introduction

The circadian rhythm is an indispensable and important factor in the host's life cycle, which enables the host metabolism regularly within 24 h [1]. The mammalian circadian clock system consists of a master clock located in the suprachiasmatic nucleus of the hypothalamus and a peripheral clock composed of organs such as the intestine, liver, and heart, etc. Through them, metabolism of the host was synchronized with the light-dark cycle [2]. Interestingly, the biological clock can improve the learning ability which depended on the hippocampus and exert a powerful influence on cognitive function [3]. Disturbance of circadian rhythm is usually accompanied by sleep disturbance, which was one of the main health problems nowadays [4]. People with circadian rhythm disorders, such as shift workers or people who frequently fly over time zones, were more likely to suffer from insomnia, depression, and neurodegenerative diseases [2]. Study using animals with knock-out specific clock genes in the system or tissue has shown that changes in the circadian rhythm can lead to abnormal metabolic phenotypes, including obesity, dyslipidemia, impaired insulin secretion, etc. [5].

In mammals, host cellular and behavioral processes showed 24 h circadian oscillations synchronized with the external light/dark cycle [6]. The gut microbiota also has circadian rhythm fluctuations, and the host circadian rhythm disturbance could affect the composition and function of the intestinal microbiota [7]. The gut microbiota was a complex micro-ecological environment, with trillions of microbes inhabiting the intestines of adults [8]. From a genetic point of view, more than 99% of human genes were microbial genes [9]. Recently research found that the loss or variation of the gut microbiota may affect neurogenesis and blood-brain barrier functions, as well as the host's cognitive function, learning ability, and emotion [10], which were partly similar to the harmful effects caused by circadian rhythm disorders. Most of the gut microbiota coexist with intestinal epithelial cells. It also acted a major role in food intake and metabolism, maintaining the intestinal barrier and the structure and function of the gastrointestinal tract [11].

Tea polyphenols can improve memory impairment caused by rhythm disorders through mechanisms related to the biological clock [12]. Epigallocatechin gallate (EGCG) is the most abundant active ingredient in tea polyphenols (TP). As the *O*-methylated form of EGCG, (-)-epigallocatechin 3-*O*-(3-*O*-methyl) gallate (EGCG3"Me), which was rich in oolong tea polyphenols (OTP) showed a potential activity similar to prebiotics [13]. OTP not only modulate the composition of the intestinal flora, but also have a positive regulatory effect on the key circadian rhythm genes in the liver [14]. Due to the low bioavailability, most OTP were metabolized by the intestinal flora into metabolic derivatives in the colon to exert biologically active functions [15]. Active metabolites can act as an intermediary between the intestine and the brain to participate in the modulation of host circadian rhythm disorders [16], but the relationship among intestinal metabolites, intestinal microbiota and rhythm genes is still unclear. Single-cell RNA

sequencing (scRNA-seq) has recently been used to understand the development and interaction of heterogeneous cells, and to detect the expression and transcription subtypes of a large number of genes throughout the genome [17]. This allows us to fairly evaluate multiple different cells and genes in the hypothalamus at the single-cell level, to better explore the link between the gut and the hypothalamus.

In this study, a mouse model of circadian rhythm disturbance was established to investigate OTP-mediated changes in intestinal microbiota, metabolites, and clock genes. Subsequently, the feces of OTP ingested mice were transplanted, and the effects of OTP intervention on mice with circadian rhythm disorders were characterized internally and externally through maze behavior experiment and hypothalamus scRNA-seq. Through fecal microbiota transplantation, a comprehensive analysis of the role of OTP in the internal and external circadian clock may provide valuable theoretical support for revealing that OTP can improve circadian rhythm disturbance *via* the GBA.

Results

Contents of tea catechins in OTP

In the present study, high purity (> 95%) of OTP was prepared (Supplementary Table S1). Results indicated that the EGCG content was the highest, making it the main tea catechin, while the content of EGCG3"Me was high.

Influence of OTP on body weight, food and water consumption of the mouse models

In Fig. S1a-c, the body weight of the constant dark group (CD group) mice increased rapidly after the first week and was higher than that of the 12 h normal light-dark cycle control group (CT group) and group under CD condition supplement with OTP (OTP group). After four weeks of OTP feeding, although the fractional body weight showed an increasing trend, it was slower than that of the CD group. The average body weight in OTP group was (23.88 ± 3.99) g, which was lower than the average body weight of the CD group mice (25.77 ± 5.09) g in the same period. Eight weeks later, the average weight of the verification group (VF group) was (27.86 ± 5.17) g. The growth rate of mice in the VF group was significantly lower than that in the CD group from the fifth week, and the body weight gradually approached the CT group ($P < 0.05$). But there was no significant difference in food and water intake during the feeding process among all groups ($P > 0.05$).

Influences of OTP on cognitive ability of mice with circadian rhythm disturbance through Y-maze and Morris water maze

In order to further observe the influence of OTP on the memory impairment caused by circadian rhythm disturbance, behavioral verification was carried out through Morris water maze and Y maze experiments. As shown in Fig. S2a, the total number of times of entering the maze arm of the three groups of mice didn't show a significant difference ($P > 0.05$). In Fig. S2b, the accuracy of spontaneous alternation of the arm in the CD group was 45.3 ± 1.6%, which was significantly lower than that of 62.8 ± 2.3% in the CT

group ($P < 0.05$). After OTP intervention, the spontaneous alternation accuracy rate of mice in the OTP group increased to 60.4 ± 3.2%. The desire to explore and short-term working memory of mice in the CD group were the weakest. The results showed that circadian rhythm disorder will damage the short-term spatial memory ability of mice, while OTP can alleviate this adverse effect, and has no obvious effect on its exercise ability.

During the water maze test, the escape latency and distance of different groups differed significantly. On the 6th day of the experiment, the escape latency to the platform for the first time was reduced to 26.0 ± 0.4 s in CD group which was significantly higher than that of the CT group (13.8 ± 0.16 s) and the OTP (16.3 ± 0.19 s) group (Fig. S3a, b). After the platform was removed, the swimming time percentages of the mice in the CT group, CD group, and OTP group in the quadrant of the original platform were 37 ± 2.0%, 24 ± 1.3%, and 30.5 ± 1.6%, respectively (Fig. S3c, d). It can be seen that the disorder of the circadian rhythm has significant negative effects on the activity state of the mice in the target quadrant, and OTP has improved this phenomenon.

The influence of OTP on the diversity of intestinal microbiota in mouse models

As shown in Table 1, the Chao1 index of all groups showed an upward trend after 4 weeks, while the CD group was significantly lower than that of the CT group and OTP group at the 4th week ($P \leq 0.05$). It showed that CD conditions significantly reduce the abundance of intestinal flora in the mouse model. After supplementing OTP, the diversity of the total microbial community increased. Both Shannon and Simpson indexes showed that the fecal microbial diversity of the OTP group was significantly higher than that of the CD group ($P \leq 0.05$). Moreover, principal coordinate analysis (PCA) showed that the fecal microbiota from the CT-4, CD-4 and OTP-4 could be separated clearly (Fig. S4).

As shown in Fig. 1a, the relative abundance of Firmicutes and Proteobacteria showed a significant downward trend after supplementing the mice with OTP for 4 weeks compared with the CD group, while the Bacteroidetes showed a significant increasing trend, and the CT group showed the same trend ($P < 0.05$). The ratio of Firmicutes/Bacteroidetes (F/B) in CD group was 158.72%, which was also significantly higher than that of 53.94% in OTP group, indicating that OTP supplementation can effectively inhibit the growth of Firmicutes and help maintain the balance of the intestinal microbiota. In addition, the number of Bacteroidetes in the CD group was significantly lower than that in the CT group (50.18 ± 20.87% vs 37.94 ± 10.69%).

The representative microflora with relative abundance at the family level were shown in Fig. 1b. Muribaculaceae belongs to the phylum *Bacteroidetes*, whose diversity provides new data for ecological research, and was named by Ilias Lagkouvardos et al [18]. After 4 weeks of feeding, the relative abundance of Muribaculaceae in the CD group was 0.06% which was significantly lower than that in the CT and OTP groups ($P < 0.05$). The relative abundance of Muribaculaceae in the CD group was significantly lower than that in the CT and OTP groups ($P < 0.05$). In particular, the relative abundance of

Lactobacillaceae reached 33.33% in the CD group, which was significantly reduced after OTP treatment ($P < 0.05$).

In order to further characterize the differences between the intestinal microbiota of mice under different treatment conditions, we performed a statistical analysis on the relative abundance of the microbiota in the samples at the genus level (Fig. 1c). Among CD-4 and OTP-4, the most significant differences were also *Bacteroides*, *Parabacteroides* and *Clostridium*. On the other hand, the relative abundance of *Muribaculum* was significantly reduced under the dark treatment for 4 consecutive weeks, and it could be increased in the OTP group ($P < 0.05$). The relative abundance of *Clostridiales*, *Lachnospiraceae*, *Eubacterium* and *Lactobacillus* in the OTP group decreased. Results showed that the intervention of OTP was beneficial under the conditions of microbial imbalance.

Effects of OTP on the diurnal oscillation of microbiota in mice with circadian rhythm disturbance

In the CT, CD and OTP groups, Firmicutes, Bacteroidetes, Proteobacteria, Tenericutes were the dominant flora at the phylum level. Different diurnal oscillation patterns of different microbiota were observed in the three groups as shown in Fig. 2a. For the CT group of mice, the main bacterial communities at the phylum level all showed obvious rhythm changes. However, the oscillation regularity of intestinal flora of mice in CD group was not strong. Interestingly, we found that OTP can significantly improve the suppression of periodic changes in phylum levels caused by continuous darkness. For example, we found that at zeitgeber time (ZT) 24, the relative abundance of Firmicutes in the CD group reached the highest, while both the CT and OTP groups were smaller than the CD group. The relative abundance of Bacteroides reached a high level at night (ZT24 and ZT48) which showed a trend higher than that of the CD group. Proteobacteria was commonly used as a microbial marker of intestinal dysregulation [19]. The relative abundance of the Proteobacteria in the OTP group was significantly lower than that in the CD group, revealing that supplementation with OTP can positively improve the diurnal oscillation of intestinal microbiota caused by circadian rhythm disturbance.

Fig. 2b analyzed the rhythmic oscillations of the intestinal microbiota of mice under different conditions at the genus level. The oscillation of *Prevotella*, *Bacteroides*, and *Parabacteroides* in the OTP group was closer to that in the CT group, and they both showed obvious rhythmic oscillation, while the oscillation of the CD group was disorder. *Prevotella* in the CT group and OTP group showed a trend of increasing during the day and decreasing at night. At ZT12, the relative abundance of *Prevotella* in the CD group was significantly lower than that in the CT group and OTP group. The relative abundance of *Bacteroides* in the CT group and OTP group reached the highest at ZT24, while the CD group reached the highest peak at ZT48.

Influences of OTP on metabolites in mice with circadian rhythm disturbance

The close grouping of QC samples in the PCA score chart further confirms the high repeatability and stability of the entire test process (Fig. S5). And the metabolites in the CT group, CD group and OTP group can be completely separated, which reflected the better quality of the data. The results showed that the

circadian rhythm disorder altered the metabolism of normal mice. The OTP group and the CT group tended to be similar, proving that OTP has a certain effect on improving the circadian rhythm disorder. In the human metabolome database (HMDB) superclass analysis, whether in positive ion mode (PIM) or negative ion mode (NIM), the most abundant metabolites belong to lipids and lipid molecules (Fig. 3a).

Metabolomics analysis was performed to determine the changes of metabolites in mice with circadian rhythm disturbance and mice after OTP intervention. The results of mass spectroscopy showed that 104 significantly different secondary metabolites were obtained under PIM and NIM conditions (53 down-regulated metabolites, 51 up-regulated metabolites) indicating significant differences in metabolites produced by OTP intervention in mice with circadian rhythm disturbance (Fig. 3b-c). Compared with the CD group, the most important characteristic after OTP intervention was a significant increase in the number of organic acids and derivatives (20 up-regulated metabolites) as well as lipids and lipid-like molecules (9 up-regulated metabolites). Especially isoleucyl-isoleucine, (R)-2-Benzylsuccinate, 4-isopropylbenzoic acid, 2-phenoxyethanol, (-)-catechin which were the top 5 significantly different metabolites by sorting in descending order of the variable influence on projection (VIP). Additionally, other metabolites associated with circadian rhythm and neuroprotection such as acetic acid, 3,4-methylenesebacic acid, hydroxyphenyllactic acid, Trp-Asn and some other metabolites were also significantly up-regulated after OTP intervention. Inversely, the levels of carcinogens o-toluidine and acylcarnitine, which can cause neurological disorders, were found to be significantly reduced after OTP supplementation indicating that OTP can reverse the metabolic disorders caused by constant dark conditions.

After the accurate analysis of the differential metabolites by the KEGG database, the pathways with significant differences in the enrichment of differential metabolites whose metabolite levels decreased significantly after treatment under constant dark conditions mainly included “glycerophospholipid metabolism”, “tryptophan metabolism”, “arginine biosynthesis”, etc. (Fig. 3d). After OTP intervened in mice living in constantly dark conditions, the differential metabolite enrichment pathway, which significantly increased the level of metabolites, was changed. As shown in Fig. 3e, the identified differential metabolite enrichment pathways were “pyruvate metabolism”, “glycolysis/gluconeogenesis”, “glyoxylate and dicarboxylate metabolism” and “tryptophan metabolism”. Pyruvate metabolism was enriched to the highest degree, and the pathway mechanism involved was shown in the Fig. 4, from which it could be seen that acetic acid was significantly up-regulated after OTP intervention.

The correlation between intestinal microbiota and intestinal differential metabolites

As shown in Fig. 5a, the microbiota most relevant to the significantly different intestinal metabolites between the CD group and OTP group were Bacteroidetes, Acidobacteria, Patescibacteria and Firmicutes. The metabolites that were significantly positively correlated with Bacteroidetes were (4-aminobutyl) guanidine, 2-phenoxyethanol, acetic acid, orcinol, isoleucyl-isoleucine, Pro-Leu, polyethylene oxidized, 3,4-methylenesebacic acid, Gln-Ile, *O*-acetyl-l-carnitine, Trp-Asn, etc ($P < 0.05$). Among them, the correlation between acetic acid, polyethylene oxidized, Gln-Ile, *O*-acetyl-l-carnitine and Bacteroidetes was extremely

significant ($P < 0.01$). Interestingly, metabolites mentioned above were negatively correlated with Firmicutes, and their significance remained unchanged. The correlation network diagram of intestinal differential metabolites and intestinal flora in the CD and OTP groups was shown in Fig. 5b, and the relationship between different phylum and metabolites can be clearly seen. The metabolites that were significantly positively correlated with Firmicutes were acylcarnitine 16:1, 2'-deoxyadenosine and agmatine ($P < 0.05$). Our data showed that intestinal flora and intestinal metabolites have a good correlation, suggesting that OTP helped the intestinal flora to repair the intestinal environment and promote the production of metabolites.

Impacts of OTP on the expression of hepatic clock genes in mouse models of circadian rhythm disorder

In order to further study the molecular mechanism of OTP affecting circadian rhythm in mice, we used transcriptome sequencing technology to perform high-throughput analysis of the peripheral clock tissue-liver. As shown in the Fig. S6, the heat map was used to reflect the expression transcription profile of liver clock genes in circadian rhythm mice within 48 h. Transcriptome data showed that 214 and 208 genes in the CT and OTP group respectively showed circadian rhythm, while only 156 genes in the CD group showed circadian rhythm. This reflected that although continuous darkness will reduce the number of clock genes in the liver of mice, the supplementation of OTP can improve this situation.

To fully grasp the expression of circadian rhythm genes, we analyzed the mRNA expression of *Bmal1*, *Clock*, *Cry1*, *Cry2*, *Per1*, *Per2*, *Per3*, *Nfil3* and *Dbp* in the liver within 48 h. As shown in the Fig. 6, most of the liver clock genes have unique circadian rhythmic expression, especially the rhythmic genes in the CT group showed a relatively regular oscillation pattern. While this regular oscillation trend did not appear well in the CD group after constant dark treatment. In particular, genes *Cry1*, *Cry2*, *Dbp*, *Per1*, *Per2* showed a distinctly different oscillation disorder from the CT group. Interestingly, even in the same environment as the constant dark treatment, the oscillation amplitude and phase of rhythmic genes (*Cry1*, *Cry2*, *Dbp*, *Per1*, *Per2*) expression began to approach the CT group after supplementing OTP. In the CT group and OTP group, the expression of genes *Bmal1* and *Nfil3* showed a downward trend during the light period (ZT12, ZT36) and an upward trend during the dark period (ZT24, ZT48). However, the genes *Cry1*, *Dbp*, *Per1*, *Per2* and *Per3* showed the opposite expression trend. The *Clock* and *Cry2* genes that lost their rhythm after dark treatment showed a regular oscillation pattern in the OTP group, although the trend was different from the CT group. At the same time, the intervention of OTP also significantly increased the oscillation amplitude of genes *Clock* and *Cry2*. All these indicated that supplementing OTP can improve the amplitude and phase shift of liver rhythm genes caused by circadian rhythm disorder to a certain extent, and make it closer to the normal level.

scRNA-seq identifies different cell clustering in the hypothalamus of mice

A total of 29,635 effective cells were detected in this experiment, of which 14,114 cells belonged to the VF group, 12,035 cells belonged to the CD group, and 3486 cells belonged to the CT group. The t-SNE clustering analysis of the above-mentioned cells in the CT, CD and VF group was performed by an automatic clustering algorithm, and the results of different samples and subgroups of cells were shown

in the Fig. 7a-b, respectively. The different colors in the picture represented different clusters and the legend on the right showed the names of each cluster. The proportion of cells in each cluster in the sample and the percentage of different sample cells in each cluster were shown in Fig. S7.

The results showed that there were 22 clusters in the CD group and 25 clusters in the VF group. After OTP intervention, the number of cells in the cluster2, cluster3, cluster4, cluster11, cluster15, cluster18, cluster19, cluster20, cluster21, cluster22, cluster23, cluster24 and cluster25 in the VF group was significantly higher than that in the CD group. Among them, the number of cells in cluster15, cluster19, cluster23, cluster24, and cluster25 in the CD group was 0, which can be used as clusters unique to OTP for cell type heterogeneity identification research.

Hypothalamus cell types and marker genes identification

The result with the highest corresponding cell type of each cluster was selected as the result of cell type identification of this cluster. The results of cell identification in the CT group, CD group and VF group were shown in Fig. 7c. The specific results of the cell types identified by each cluster and their percentages were shown in Table S2. As shown in Fig. 7d, the cell types of the two groups of samples were annotated respectively, and the heterogeneity of the expression of each cell type in the two groups of samples could be clearly and intuitively seen. The main cell types identified by the CD group and VF group of samples included astrocytes, oligodendrocytes, microglia, macrophages, neurons, epithelial cells, endothelial cell, and fibroblast. Fibroblasts only uniquely existed in the VF group, but not in the CD group.

We focused on the analysis of cluster15, cluster19, cluster23, cluster24, and cluster25 to determine the cell heterogeneity between the CD group and the VF group. Cluster15 and cluster25 were identified as oligodendrocytes, which acted an indispensable role in neuron protection and development [20], and the number of cells in the VF group was significantly higher than that in the CD group. In cluster19, 79.11% were identified as oligodendrocytes, 16% were neurons, and 4.89% were astrocytes which were important parts of the central nervous system cells. Cluster23 and cluster24 were identified as macrophages and fibroblasts, respectively. After fecal bacteria transplantation, the number of these cells in the hypothalamus was significantly increased.

Circadian rhythm genes expression of each cell types in and around the hypothalamus

The expression of marker genes in each cluster was shown in Fig. S8, the high expression of different marker genes reflected the unique genes in each cluster. The average gene expression profiles of 30,691 gene samples that were common in 8 cells was shown in Table S3.

We selected a total of 16 co-expressed rhythmic genes (*Clock*, *Bmal1*, *Cry1*, *Cry2*, *Per1*, *Per2*, *Per3*, *Bhlhe41*, *Nr1d1*, *Nr1d2*, *Dbp*, *Rorb*, *Tim*, *Dbt*, *Sirt*, *Nfil3*) from the top 8 major cell types, which were mainly core clock genes and genes involved in coding clock gene proteins. The expression levels of circadian genes in fibroblasts, epithelial cells, endothelial cell, neurons and astrocytes were relatively high (Fig. S9a). Moreover, the expression level in VF group was higher than that in CD group, especially the percent

expressed ratio of rhythm genes *Cry2*, *Per3*, *Bhlhe41*, *Nr1d1*, *Nr1d2*, *Dbp*, *Rorb* in each cell in the VF group (Fig. S9b).

The specific expression of circadian rhythm genes in each cell and different groups was shown in Fig. 8a. The percent expressed ratio and average expression of the rhythm gene *Clock* in the neurons of the VF group were the highest. Although the percent expressed ratio of *Clock* in oligodendrocytes in the VF group was similar to that of neurons, the average expression was much lower than neurons. Meanwhile, it was found that the average expression of other rhythm genes *Clock, Bmal1*, *Cry1*, *Per2*, *Per3*, *Nr1d2*, *Dbp* and *Rorb* in neurons of the VF group was also relatively high. The t-SNE map was used to cluster and identify the expression patterns of circadian rhythm genes in neurons of the CD and VF group, as shown in Fig. 8b. From the t-SNE graph of gene expression, it can be reflected that *Clock*, *Cry2*, *Per3*, *Bhlhe41*, *Nr1d1*, *Nr1d2*, *Dbp* and *Rorb* have a relatively high expression ratio in neurons in the VF group. From this we speculate that neurons were one of the main cells expressing circadian rhythm genes, which was consistent with the findings of Branchaccio et al [20]. And OTP can enhance the expression of circadian rhythm genes in them.

The violin plot can clearly show the expression of circadian rhythm genes in each cell in the hypothalamus (Fig. 8c). Compared with the CD group, the *Clock*, *Cry2*, *Per3*, *Bhlhe41*, *Nr1d1*, *Nr1d2*, *Dbp* and other genes related to the circadian rhythm in the VF group were better expressed in each cell. In the CD group, the top 3 cells with the expression levels of the core clock genes *Clock* and *Bmal1* were astrocytes, oligodendrocytes and epithelial cells. While in the VF group, the top 3 cells with the *Clock* expression levels were astrocytes, neurons and epithelial cells. The top 3 cells with *Bmal1* expression level in the VF group were consistent with the CD group.

Gene Ontology (GO) and KEGG analysis of different expression genes (DEGs) in liver and hypothalamus

The results of liver transcriptome sequencing showed that after 4 weeks of OTP intervention, GO terms enriched in the biological process mainly included “negative regulation of transcription by RNA polymerase II”, “regulation of transcription, DNA-templated” and “negative regulation of transcription, DNA-templated”. It showed that OTP could improve the effects of continuous darkness by affecting the biological process of the host. The cellular components were mainly enriched in “nucleus”, “cytoplasm”, and “membrane” etc. Among the molecular functions were “protein binding”, “metal ion binding”, and “DNA binding” etc (Fig. 9a). In organisms, different expression genes (DEGs) coordinate with each other to perform their biological functions. On the basis of GO annotation classification, KEGG analysis was used to enrich the results for biological pathway analysis [21]. Comparing the two groups of CD and OTP, 396 unigenes were annotated in the KEGG database and mapped to 191 metabolic pathways. Among them, “circadian rhythm”, “ubiquinone and other terpenoid-quinone biosynthesis” and “fatty acid elongation” were highly enriched in KEGG pathways which were closely related to the perfection of circadian rhythms and protein phosphorylation *in vivo* (Fig. 9b).

As shown in Fig. 9c, the top 3 in the biological process field in hypothalamus were mainly “positive regulation of transcription by RNA polymerase II”, “multicellular organism development”, and “signal

transduction". In terms of cellular component, "membrane", "cytoplasm", and "nucleus" were mainly involved. The main processes in molecular function were "protein binding", "metal ion binding", and "nucleariide binding" which were highly similar to the GO analysis results of liver sequencing. After fecal microbiota transplantation, the DEGs involved in the KEGG pathways between the CD group and VF group have become richer. Mainly reflected in "human diseases", "metabolism" and "organismal systems" as shown in Fig. 9d. According to the degree of gene enrichment in each category, the top 3 pathways associated with "human diseases" were "neurodegenerative disease", "infectious disease: parasitic" and "endocrine and metabolic disease". There were "energy metabolism" (25 DEGs), "lipid metabolism" (28 DEGs) and "carbohydrate metabolism" (26 DEGs) that have a higher percentage of gene expression in "metabolism". In the "organismal systems" category, there were "nervous system", "endocrine system", and "immune system" where the number of DEGs expression distributions was more than 60, the proportion of the number of DEGs expressions in the total gene expression of the them were rose to 14.01%, 8.81% and 7.66%, respectively.

Table 1. Effects of OTP on the biodiversity of gut microbiota in the circadian rhythm disorder mice model.

Sample	Chao1	Shannon	Simpson
CT-0	578.26±26.33^{a}	4.23±0.15^{b}	0.85 ± 0.02^{b}
CT-4	724.63±23.89^{d}	4.72±0.23^{d}	0.81±0.02^{a}
CD-0	572.24±21.83^{a}	4.24±0.14^{b}	0.86±0.03^{b}
CD-4	586.03±32.17^{b}	4.18±0.17^{a}	0.87±0.03^{b}
OTP-0	575.21±21.15^{a}	4.22±0.13^{b}	0.86±0.02^{b}
OTP-4	635.83±28.56^{c}	4.61±0.18^{c}	0.82±0.02^{a}

Different letters in the same column indicate significant differences ($P < 0.05$) among different samples.

Discussion

As a basic component of the living body, the circadian rhythm is an endogenous and guidable biological process [22]. Each cell of the host contained an internal biological clock, which performed normal turnover *via* a series of rhythmic genes or molecular oscillations [23]. Irregular lifestyle and diet or circadian rhythm disorders caused by long-term shift work may cause the host's central-peripheral circadian clock disorder and increase the risk of neurodegenerative diseases, cognitive impairment and other metabolic diseases [24]. The study by Thaiss et al. [6] found that transplanting the gut microbiota with jet lag into mice resulted in a significant increase in host fat. In our research, it was found that after transplanting the intestinal flora of mice supplemented with OTP into mice with circadian rhythm disorders, the weight of the mice increased extremely slowly and approached mice living in a normal

environment. This showed that the intake of OTP can improve the negative response of circadian rhythm disorders to weight.

The host's circadian rhythm pattern can be measured by biological and behavioral indicators. The activity-rest cycle is the characteristic that we spend 24 h a day inducing physiological and cellular adaptation to various processes [25]. In addition to having the extensive effects on physiology, the circadian rhythm also affects the host's learning and memory abilities. Similar to the cognitive impairment of mice with circadian rhythm disorders observed in this experiment, study has shown that mice with disrupted circadian rhythm genes also showed poor performance in various learning behavior tasks [26]. Similarly, the disturbance of humans' circadian rhythm can also lead to the decline of cognitive function. For example, flying across time zones for several years would increase the cognitive impairment of the host [27]. Four weeks after supplementing the OTP, the long-term cognitive learning impairment assessed in the Morris water maze and the short-term memory impairment in the Y-maze were reversed. This phenomenon was similar to the findings of Biasibetti et al. [28] that tea catechins can reduce oxidative stress in peripheral and brain tissues and inhibit behavioral changes related to cognitive deficits.

Previous study by others has indicated that disruptions in circadian rhythm led to variations in gut microbiota characterized by an increase in pro-inflammatory bacteria and a decrease in bacteria which produce anti-inflammatory short-chain fatty acids (SCFAs) [29]. In this study, we observed that the value of F/B was higher than that of normal mice in mice with circadian rhythm disorders. After OTP intervention, the ratio of F/B in the gut microbiota of mice with circadian rhythm disorders decreased, and Bacteroidetes increased significantly. Additionally, supplementation of OTP for 4 weeks also significantly increased the relative abundance of Muribaculaceae which was belong to Bacteroidetes. The relatively high relative abundance of Muribaculaceae (previously named S24-7) was related to the extension of lifespan [30]. Muribaculaceae has been also reported to contribute to the production of SCFAs [31]. SCFAs were the main metabolites of the gut microbiota. As signal molecules, SCFAs can activate multiple pathways, such as activating AMP-activated protein kinase in peripheral tissues (such as liver and muscle) and cholesterol or lipids metabolism etc. [32]. Additionally, studies have shown that SCFAs may affect cognitive function and mood through a variety of mechanisms, included regulation of histone acetylation and methylation, promotion of secretion of various hormones and neurochemicals (such as serotonin), and induction of vagal nerve signals [33, 34]. It was observed that the relative abundance of acetate and butyrate-producing bacteria in mice supplemented with OTP showed an increasing trend in our research.

Metabolites can drive the relationship between the host and microbiota. At the same time, metabolites were considered to be cellular transmitters of circadian rhythms in various tissues [35]. Microbial-derived SCFAs or lactate were found to regulate the phase of the host's peripheral clock *in vivo* [36]. Trp is a dietary essential amino acid, which can be directly metabolized in the gastrointestinal tract through the microbiota or serotonin pathway and transmit signals from the intestine to endogenous or exogenous neurons [37]. The metabolism of tryptophan by the microbiota included the conversion of tryptophan to

indole and its derivatives, of which 5-Hydroxyindole-3-acetic acid (5-HIAA) is main metabolite [37]. The enrichment pathways that significantly down-regulated differential metabolites in the CD group included tryptophan, glycerophospholipid metabolism, etc. Study has shown that phospholipid compounds involved in glycerophospholipid metabolism participate in diseases such as atherosclerosis, vascular dementia, and spinal cord injury by activating the PPARγ pathway [38]. Choline is a strong organic base that exists in sphingomyelin and can be used as a precursor of the neurotransmitter acetylcholine [39]. The content of choline and 5-HIAA in mice that have lived in constantly dark conditions for a long period has a downward trend which indicated that the disorder or destruction of the circadian rhythm may affect the synthesis and transport of neurotransmitters, etc.

The activity of TP depended largely on its conversion in the intestine [40]. Due to the limited bioavailability of TP in the body, most of TP exerted functionally activities by their metabolic derivatives [13]. In this study, OTP and its metabolites have shown various positive effects on metabolic disorders caused by circadian rhythm disorders. After OTP intervention in mice with circadian rhythm disorders, the content of multiple metabolites which originally were have a down-regulated trend in CD group was now significantly increased, and tended to the level of the CT group. Some representative metabolites were screened out, such as acetic acid, (-)-catechin, O-acetyl-L-carnitine, 2-indolecarboxylic acid, 3-hydroxy-3-methylglutaric acid, etc. The protein kinase C-related properties of catechins make it have a positive impact on the anti-neurodegenerative disease Alzheimer's disease [41]. The metabolic levels of various amino acids such as tryptophan, glutamine (Gln), alanine, and tyrosine (Tyr) were significantly increased after OTP supplementation. Metabolic syndrome and neurological features (significantly anxiety, depression, and autism), were mostly affected by the final product of tryptophan metabolism [37]. 2-indolecarboxylic acid was one of the tryptophan pathways and has been found to be involved in immune regulation, inflammation and affect intestinal function [42]. Gln can effectively enhance the function, proliferation and life cycle of small intestinal epithelial cells, and may indirectly support the optimal neuropsychological environment by protecting the intestinal wall from damage and chronic inflammation [43]. In another study, after long-term supplementation of Gln, the ratio of F/B, a common indicator of obesity, was significantly reduced. An optimized intestinal microecological environment was more likely to perform neurotransmitter synthesis and other functions more effectively [44]. Tyr was also a precursor of neurotransmitters formation, and the increase of Tyr can increase the level of neurotransmitter in the body [45]. The supplementation of OTP can increase the level of Gln and Tyr. An optimized intestinal microecological environment was more likely to perform neurotransmitter synthesis and other functions more effectively. Abnormal “pyruvate metabolism” often leads to cancer, heart failure and neurodegenerative diseases. KEGG enrichment analysis of differential metabolites significantly up-regulated after OTP intervention showed that the degree of enrichment of "pyruvate metabolism" was the highest which can be explained that the intervention of OTP is beneficial to the reversal of these abnormal phenomena [46].

The liver and intestine were both typical peripheral clock models in the biological clock system. They were synchronized with the circadian rhythm of the central clock in the suprachiasmatic nucleus (SCN) and affected by meal time and dietary composition [47]. The supplementation of OTP can increase the

number of rhythmic genes in the liver of mice and positively improved the disorder of the expression patterns of liver clock genes. The microbiota with circadian rhythm oscillations accounts for about 60% of the gut microbiota [6]. And in this study, compared with the microbial population that normally undergoes the light-dark cycle, constant darkness changed the oscillation of some microbes, and this situation can be significantly alleviated by supplementing OTP. KEGG analysis showed that DEGs obviously have the highest levels in “protein processing in endoplasmic reticulum”, “endocytosis”, and “MAPK signaling pathway” after OTP supplementation. It can be seen that after OTP interferes with mice with circadian rhythm disorders, cell transcription and translation activities become active, and can regulate circadian rhythm disorders by participating in the formation of proteins.

Circadian rhythm can be found at the intracellular level and is coordinated by the SCN master clock located in the hypothalamus [48]. Patients with different degrees of Alzheimer's disease were considered to have circadian rhythm disorders, which were specifically manifested as delayed attenuation of amplitude and phase [49]. The lack or disorder of clock gene expression in astrocytes can lead to neuroinflammation which was the main manifestation factor of neurodegeneration[3]. For instance, the absence of *Bmal1* in the mouse brain disrupted the function of the biological clock and also caused the degeneration of the synapses of astrocytes [50]. Astrocytes can selectively remove synapses, fine-tune and reshape the brain's neural circuits during host learning, memory and exercise [48]. It has been confirmed that transplantation of human astrocytes into newborn mice can enhance the memory and learning ability of mice [51]. It has been confirmed that transplantation of human astrocytes into newborn mice can enhance the memory and learning ability of mice [52]. Oligodendrocytes provided metabolic support and nerve repair functions for neurons and axons, which were thought to be related to some mental diseases [53]. Neurons have always been considered a crucial part of SCN. The latest research shows that neurons can not only participate in the regulation of clock gene expression and maintain circadian rhythmic oscillations to coordinate the biological clocks of tissues and organs throughout the body, but also have the ability to autonomously encode circadian rhythms, so as able to initiate and maintain biological rhythmic activities and behaviors [20]. Among the 8 hypothalamic cell types identified in this study, we revealed that fibroblasts only exist in the VF group, and the number of astrocytes and oligodendrocytes was up-regulated. Rhythmic genes such as *Clock*, *Cry2*, *Per3*, *Bhlhe41*, *Nr1d1*, *Nr1d2*, *Dbp*, etc. showed better expression after OTP intervention. Notably, the expression percentage and average expression level of the rhythm gene *Clock* in the VF group neurons were both the highest. All these supports the perspective that OTP can improve the negative effects of circadian rhythm disorders by increasing the number of cells and gene expression associated with the circadian rhythms.

The functional enrichment analysis of significantly differential gene expression in hypothalamic cells can further support the above viewpoints. GO classification analysis suggested that OTP supplementation may ameliorate the negative effects of circadian disruption by altering cell composition [54]. The mechanism by which TP participate in the intestinal microbiota and its metabolism to regulate circadian gene expression includes the interaction of the basic development and metabolism of the microbiota, as well as interference with cell membrane function and energy metabolism [55]. KEGG pathway analysis

showed that after fecal microbiota transplantation, DEGs were mainly enriched in “signal transduction”, “cancer: overview”, “nervous system” and “endocrine system”. These pathways were closely associated with the health of the host.

Conclusions

In this study, the intervention of OTP reduced the F/B ratio, the daily oscillation of the intestinal microbiota tended to be regular, and the intestinal microecological status was also better than that in the CD environment. After OTP mediated, the content of important metabolic targets closely associated with host metabolism such as Trp, Gln, Thr, Pro, alanine, 2-indolecarboxylic acid and some others has been significantly increased. The poor expression of liver clock genes has been improved, KEGG analysis showed that the significance differences between the OTP group and CD group were in “signal transduction”, “endocrine system”, “cancer: overview” and “immune system”, etc. After fecal microbiota transplantation in the OTP group, the expression percentages of most rhythm genes such as *Cry2, Per3, Bhlhe41, Nr1d1, Nr1d2, Dbp* and *Rorb* were higher in hypothalamus cells than those in the constant dark environment. Behavioral experiments confirmed that the short-term and long-term cognitive learning abilities of mice after fecal microbiota transplantation were better than those in the CD group. These results indicated that OTP can significantly improve the metabolic imbalance caused by the circadian rhythm disorder, maintain the host's homeostasis, and improve cognitive ability.

Materials

Chemicals and Reagents

Oolong tea was produced in Baifeng Tea Garden, Beilun District, Ningbo City, Zhejiang Province. Polyamide resin was purchased from Ocean Chemical Co., Ltd. (Qingdao, China). Sterile male mice C57BL/6J were purchased from Hunan Slack Experimental Animal Co., Ltd. Ordinary animal feed is provided by the Experimental Animal Center of Ningbo University.

Preparation of OTP

The dried sample was ground into a powder with a grinder, and the material passing through a 40-mesh sieve was stored in a sealed polyethylene bag at a temperature of 20 °C until use. Shortly, take the tea powder and add distilled water, and place it at 96 °C for 40 min. The extract was centrifuged at 4500 *g* for 15 min. Repeat the above process. According to the method we previously reported, the residue is dissolved, sorted and purified through a polyamide column. The eluate was analyzed using high performance liquid chromatography [56]. And collect, concentrate, load on the polyamide column and process the required fractions as described above. The results showed that the components containing OTP were concentrated and freeze-dried through a freeze-drying system to obtain finished products.

Animals and experimental design

Animal studies were carried out in the Centre for Laboratory Animals, Ningbo University (Permission No. SYXK [Zhejiang] 2013-0191). All the animal-related operations were strictly in compliance with the relevant laws and regulations on the use and care of laboratory animals in China. All mice were individually placed in a sterile barrier environment with a room temperature of 22.3 °C and a humidity of 55.5%. Adapt to the environment for 7 days under a 12h light-dark cycle period [ZT0 = 6 am, lights on; ZT12 = 6 pm, lights off]. Seven days later, they were randomly divided into 4 groups (18 animals in each group), namely CT group, CD group, VF group and OTP group. The CT group continued to grow in a 12 h light-dark cycle environment, the CD and VF group was placed in a completely dark environment, and the OTP group was placed in a completely dark environment and fed with 0.1% (w/w) OTP once a day [54]. At the same time, the CT, CD and VF group were given the same amount of sterile water per day. The body weight, water and food consumption of CT, CD, OTP and VF group of animals were recorded every week. After 4 weeks of continuous administration, laparotomy was conducted on 3 mice of CT, CD and OTP group under pentobarbital anesthesia every 12 h over 48 h, which can be divided into 5 groups according to time points and fresh feces were collected respectively for intestinal microbiota analysis. The liver and contents of the cecum were collected immediately after euthanasia for analysis of clock genes and differential metabolites.

After sampling, the intestinal flora of the remaining 3 mice in the OTP group were transplanted into the mice in the VF group for subsequent verification tests. Briefly, fresh fecal samples from the OTP group collected in the 4^{th} week as abovementioned were mixed with sterile saline and centrifuged at 3000 *g* for 5 min. The supernatant was collected and homogenized into 400 mg/mL faecal liquid, and gavage once a day 0.2 mL last 1 week [57]. The remaining mice in the CT and CD groups group were given the same amount of sterile water per day continue to be cultured for 4 weeks until the eighth week under the original culture conditions. After 8 weeks, conduct animal behavior experiments and repeat the above anesthesia operation to euthanize the mice, and then remove the hypothalamus.

Animal Behavioral Tests

The Y-maze spontaneous alternation experiment was mainly used to evaluate the short-term working memory ability of mice. Five mice in each group were randomly selected for maze test. After 1 h of dark adaptation, all mice were put into the center of the Y-maze device and explored freely in the Y-maze for 8 min. Record the arm-in sequence and the total number of arm-in-arms to calculate the correct rate of spontaneous alternation. Entering three different arms in a row was the correct alternate response. The correct rate of spontaneous alternation = [the number of correct spontaneous alternation / (total number of arm advance - 2)] × 100% [58].

The MWM test was a classic experiment to test the long-term spatial learning and memory ability of mice, and it was also one of the most widely used tests in behavioral neuroscience [59]. The MWM experiment was completed in a total of 6 days. During the experiment, the water temperature was maintained at 20-25 °C. On the first day, the water was colorless, the platform was clearly visible and each group of mice swam freely in the maze for 90 s to adapt to the environment. Non-toxic food-grade titanium dioxide was

added to the water on day 2 to 6 until the water became opaque and white in order to clearly record the movement of the mice. The escape platform (set in quadrant II) is hidden 0.5-1.0 cm below the water surface, and put the mice into the maze from quadrants Ⅰ, Ⅲ and IV each time so that they can freely search for the platform within 60 s. On the 6^{th} day, the time and trajectory of each group of mice reaching the platform (set in the II quadrant) were recorded. Then remove the platform, record the swimming time and trajectory of the mouse within 60 s in the quadrant where the original escape platform was located (quadrant II), and calculate the percentage of the mouse's swimming time in the target quadrant. These data were measured by photoelectric sensors and analyzed using a video tracking system connected to a computer (SuperMaze software, Shenzhen Rayward Life Technology Co. Ltd, China).

DNA extractions and Intestinal Microbiota Analysis

DNA extraction and high-throughput sequencing were performed based on the methods we reported earlier, and some of the procedures were modified appropriately [14]. DNA from different samples was extracted using the E.Z.N.A. ®Stool DNA Kit (D4015, Omega, Inc., USA) according to manufacturer's instructions. The 5' ends of the primers were tagged with specific barcods per sample and sequencing universal primers. Prior to sequencing, the V3-V4 (5'-CCTACGGGNGGCWGCAG-3', 5'-GACTACHVGGGTATCTAATCC-3') variable region of each sample was amplified with a set of universal primers targeting the 16S rRNA gene region. The size and quantity of the amplicon library were assessed on Agilent 2100 Bioanalyzer (Agilent, USA) and with the Library Quantification Kit for Illumina (Kapa Biosciences, Woburn, MA, USA), respectively. The libraries were sequenced on NovaSeq PE250 platform. The combined pair sequences were analyzed using the QIME (Quantitative Insights Into Microot Ecology) (version 1.2.8) software package [60], and high quality reads were collected into the operational classification unit for subsequent analyses [61].

Metabolite extraction and Metabolomics data processing

Based on the research method of Qiu et al., [62] metabolites were extracted from the cecal content of CT, CD, and OTP groups for metabolomics analysis. The frozen cecal contents were crushed with liquid N_2 and thawed on ice. The precooled 50% methanol buffer was mixed with the thawed samples at a ratio of 6:1, vortexed for 1min and incubated at room temperature for 10min, followed by overnight storage at -20 °C. After centrifugation, the supernatant was transferred to 96-well plates and stored at -80 °C for LC-MS analysis.

The ultra-performance liquid chromatography (UPLC) system (SCIEX, UK) was used for chromatographic separation. The reversed-phase separation adopts ACQUITY UPLC T3 column (100mm*2.1mm, 1.8mm, Waters, UK), the column temperature is 35℃, and the mobile phase and flow rate refer to the recommendations of Want et al. [63]. The eluted metabolites were detected using the TripleTOF 5600 Plus system (SCIEX, Warrington, UK) [64]. XCMS software was used to preprocess the obtained mass spectrometry data. The open databases KEGG and HMDB were used to compare and annotate metabolites. The selected differential metabolites were imported into the pathway analysis module in the

MSEA (Metabolite Set Enrichment Analysis) software (https://www.metaboanalyst.ca/MetaboAnalyst/faces/home.xhtml) to match.

mRNA library sequencing and transcription abundance analysis of liver genes

Use TRIzol (Invitrogen, CA, USA) to separate and purify the RNA from mouse liver samples according to the operating protocol provided by the manufacturer. Then use Bioanalyzer 2100 (Agilent, CA, USA) and NanoDrop ND-1000 (NanoDrop, Wilmington, DE, USA) to analyze the amount and purity of total RNA. In order to reduce the impact of sequencing depth and gene length on the number of reads, we calculated the transcript expression level of each gene through the transcript splicing comparison ranking index (HISAT), and normalized it to map per million fragments per thousand base transcripts (FPKM) fragment which were defined the expression level of mRNA.

Single cell preparation and scRNA-seq

The hypothalamus of mice (0.2-0.9 g) was transferred from cardioplegic solution into gentle MACS C-tubes (Miltenyi Biotec). Hypothalamus were minced using scissors (FST) and automatically digested using gentle MACS Octo Dissociator (Miltenyi Biotec) with heaters. Cardiomyocyte-depleted single-cell suspension were washed with base solution containing 20% fetal bovine serum (FBS, Gibco), then filtered and centrifugation and resuspended in base solution containing 0.2% FBS (Gibco). Single cells were processed using Chromium Controller (10X Genomics) according to the manufacturer's protocol, then prepared through a library preparation by LC Sciences. Post-processing and quality control using 10X Cell Ranger package (v1.2.0; 10X Genomics).

Bioinformatic analysis of scRNA-Seq Data

Bioinformatic analysis of scRNA-seq were conducted by LC-bio (Hangzhou. China), and the R package Seurat (version 3.0) with default parameters was used to further analyze the expressed genes. Clustering analysis was carried out with standard seurat package procedures with a resolution at 1.2. In order to identify unbiased cell types of sRNA-seq, we used single-cell transcriptomics R to annotate cell clusters and compared them with the immune genome project (reference mouse data set) [65]. In order to further determine the enrichment process in clustering, we used Original Path Analysis (IPA) to analyze the enrichment pathway [66]. The top GO package in R (Bioconductor) was used for gene ontology (GO) enrichment analysis, and the Clue GO plug-in of Cytoscape software was used for KEGG pathway enrichment analysis [67].

Statistical analysis

The data obtained in this study were analyzed by SPSS (SPSS Inc., Chicago, IL, USA, v 17.0.0). Comparison between groups was performed using one-way analysis of variance (ANOVA) with the *post hoc* Tukey test for multiple comparisons. $P < 0.05$ was considered to be statistically significant.

Declarations

Ethics approval and consent to participate

Animal studies were carried out in the Centre for Laboratory Animals, Ningbo University (Permission No. SYXK [Zhejiang] 2013-0191). All the animal-related operations were strictly in compliance with the relevant laws and regulations on the use and care of laboratory animals in China.

Authors' contributions

RY and XZ drafted the manuscript. RY and XZ performed the animal's test and supervised the work. RY, CH, YL, and RZ analyzed the metabolomics data. RY, ZW, and PW performed the 16S rRNA sequencing and analysis. RY, CH, YL, and RZ analyzed the RNA sequencing data. RY and XZ conducted the statistics study. All authors critically revised the manuscript. All authors read and approved the final manuscript.

Acknowledgements

The authors would like to thank Hangzhou LC-Bio Technology Co., Ltd for the sequencing service.

Funding

This work was sponsored by Zhejiang Provincial Natural Science Foundation of China (LY19C200006), Zhejiang Provincial Key Research and Development Program (2020C02037) and People-benefit Project of Ningbo (202002N3078).

Consent for publication

Not applicable.

Competing interests

The authors have declared no conflict of interest.

Availability of data and materials

All data generated or analyzed during this study are included in this published article [and its supplementary information files].

References

1. Husse J, Eichele G, Oster, H. Synchronization of the mammalian circadian timing system: light can control peripheral clocks independently of the SCN clock: alternate routes of entrainment optimize the alignment of the body's circadian clock network with external time. BioEssays 2015; 37: 1119-1128.

2. Yan RN, Ho C-T, Zhang X. Interaction between tea polyphenols and intestinal microbiota in host metabolic diseases from the perspective of the gut-brain axis. Mol Nutr Food Res. 2020; 64: 2000187.

3. Musiek ES, Holtzman DM. Mechanisms linking circadian clocks, sleep, and neurodegeneration. Science. 2016; 354: 1004-1008.

4. Goel N, Basner M, Rao H, Dinges DF. Circadian rhythms, sleep deprivation, and human performance. Prog Mol Biol Transl Sci. 2013; 119: 155-190.

5. Dallmann R, Viola AU, Tarokh L, Cajochen C, Brown SA. The human circadian metabolome. Proc Natl Acad Sci USA. 2012; 109: 2625-2629.

6. Thaiss CA, Zeevi D, Levy M, Zilberman-Schapira G, Suez J, Tengeler AC, Abramson L, Katz MN, Korem T, Zmora N, et al. Transkingdom control of microbiota diurnal oscillations promotes metabolic homeostasis. Cell. 2014; 159: 514-529.

7. Thaiss CA, Levy M, Korem T, Dohnalová L, Shapiro H, Jaitin DA, David E, Winter DR, Gury-BenAri M, Tatirovsky E, et al. Microbiota diurnal rhythmicity programs host transcriptome oscillations. Cell. 2016; 167: 1495-1510.

8. Gentile CL, Weir TL. The gut microbiota at the intersection of diet and human health. Science. 2018; 362: 776-780.

9. Wu JY, Wang K, Wang XM, Pang YL, Jiang CT. The role of the gut microbiome and its metabolites in metabolic diseases. Protein Cell. 2021; 12: 360-373.

10. Vuong HE, Yano JM, Fung TC, Hsiao EY. The microbiome and host behavior. Annu Rev Neurosci. 2017; 40: 21-49.

11. Jandhyala SM, Talukdar R, Subramanyam C, Vuyyuru H, Sasikala M, Reddy DN. Role of the normal gut microbiota. World J Gastroenterol. 2015; 21: 8787-8803.

12. Qi GY, Mi YS, Liu ZG, Fan R, Qiao QL, Sun YL, Ren B, Liu XB. Dietary tea polyphenols ameliorate metabolic syndrome and memory impairment via circadian clock related mechanisms. J Funct Foods. 2017; 34: 168-180.

13. Zhang M, Zhang X, Ho C-T, Huang QR. Chemistry and health effect of tea polyphenol (-)-epigallocatechin 3-O-(3-O-Methyl) gallate. J Agric Food Chem. 2019; 67: 5374-5378.

14. Guo TT, Ho C-T, Zhang X, Cao JX, Wang HF, Shao XF, Pan DD, Wu ZF. Oolong tea polyphenols ameliorate circadian rhythm of intestinal microbiome and liver clock genes in mouse model. J Agric Food Chem.2019; 67: 11969-11976.

15. Zhang, X. Chen YH, Zhu JY, Zhang M, Ho C-T, Huang QR, Cao JX. Metagenomics analysis of gut microbiota in a high fat diet-induced obesity mouse model fed with (-)-epigallocatechin 3-O-(3-O-Methyl) Gallate (EGCG3"Me). Mol Nutr Food Res. 2018; 62: e1800274.

16. Hou QQ, Zhang SM, Li Y, Wang HJ, Zhang D, Qi DM, Li YL, Jiang HQ. New insights on association between circadian rhythm and lipid metabolism in spontaneously hypertensive rats. Life Sci. 2021; 271: 119145.

17. Hwang B, Lee JH. Bang D. Single-cell RNA sequencing technologies and bioinformatics pipelines. Exp Mol Med. 2018; 50: 1-14.

18. Lagkouvardos I, Lesker TR, Hitch TCA, Gálvez EJC, Smit N, Neuhaus K, Wang J, Baines JF, Abt B, Stecher B, et al. Sequence and cultivation study of Muribaculaceae reveals novel species, host preference, and functional potential of this yet undescribed family. Microbiome. 2019; 7: 28.

19. Shin NR, Whon TW, Bae JW. Proteobacteria: microbial signature of dysbiosis in gut microbiota. Trends Biotechnol. 2015; 33: 496-503.

20. Brancaccio M, Edwards MD, Patton AP, Smyllie NJ, Chesham JE, Maywood ES, Hastings MH. Cell-autonomous clock of astrocytes drives circadian behavior in mammals. Science. 2019; 363(6423):187-192.

21. Kanehisa M, Goto S. KEGG: kyoto encyclopedia of genes and genomes. Nucleic Acids Res. 2000; 28: 27-30.

22. Dunlap JC, Loros JJ. Yes, circadian rhythms actually do affect almost everything. Cell Res. 2016; 26: 759-760.

23. Yamazaki S, Numano R, Hida MAA, Takahashi R, Ueda M, Block GD, Sakaki Y, Menaker M, Tei H. Resetting central and peripheral circadian oscillators in transgenic rats. Science. 2020; 288: 682-685.

24. Parkar SG, Kalsbeek A, Cheeseman JF. Potential role for the gut microbiota in modulating host circadian rhythms and metabolic health. Microorganisms. 2019; 7: 41.

25. Duclos C, Dumont M, Jean P, Blais H, der Maren SV, Menon DK, Bernard F, Gosselin N.Sleep-wake disturbances in hospitalized patients with traumatic brain injury: association with brain trauma but not with an abnormal melatonin circadian rhythm. Sleep. 2020; 43: zsz191.

26. Wang LMC, Dragich JM, Kudo T, Odom IH, Welsh DK, O'Dell TJ, Colwell CS. Expression of the circadian clock gene Period2 in the hippocampus: possible implications for synaptic plasticity and learned behaviour. ASN Neuro.2009; 1: e00012.

27. Cho K. Chronic 'jet lag' produces temporal lobe atrophy and spatial cognitive deficits. Nat Neurosci. 2001; 4: 567-568.

28. Biasibetti R, Tramontina AC, Costa AP, Dutra MF, Quincozes-Santos A, Nardin P, Bernardi CL, Wartchow KM, Lunardi PS, Gonçalves CA. Green tea (-) epigallocatechin-3-gallate reverses oxidative stress and reduces acetylcholinesterase activity in a streptozotocin-induced model of dementia. Behav. Brain Res. 2013; 236: 186-193.

29. Voigt RM, Forsyth CB, Green SJ, Mutlu E, Engen P, Vitaterna MH, Turek FW, Keshavarzian A. Circadian disorganization alters intestinal microbiota. PLoS One. 2014; 9: e97500.

30. Piao SH, Zhu ZQ, Tan SY, Zhan HX, Rong XL, Guo J. An integrated fecal microbiome and metabolome in the aged mice reveal anti-aging effects from the intestines and biochemical mechanism of FuFang zhenshu TiaoZhi (FTZ). Biomed. Pharmacother. 2020; 121: 109421.

31. Smith BJ, Miller RA, Ericsson AC, Harrison DC, Strong R, Schmidt TM. Changes in the gut microbiome and fermentation products concurrent with enhanced longevity in acarbose-treated mice. BMC Microbiol. 2019; 19: 130.

32. den Besten G, van Eunen K, Groen AK, Venema K, Reijngoud DJ, Bakker BM. The role of short-chain fatty acids in the interplay between diet, gut microbiota, and host energy metabolism. J Lipid Res. 2013; 54: 2325-2340.

33. Arnoldussen IAC, Wiesmann M, Pelgrim CE, Wielemaker EM, van Duyvenvoorde W, Amaral-Santos PL, Verschuren L, Keijser BJF, Heerschap A, Kleemann R, et al. Butyrate restores HFD-induced adaptations in brain function and metabolism in mid-adult obese mice. Int J Obes. 2017; 41: 935-944.

34. van de Wouw M, Boehme M, Lyte JM, Wiley N, Strain C, O'Sullivan O, Clarke G, Stanton C, Dinan TG, Cryan JF. Short-chain fatty acids: microbial metabolites that alleviate stress-induced brain-gut axis alterations. J Physiol. 2018; 596: 4923-4944.

35. Eckel-Mahan KL, Patel VR, Mohney RP, Vignola KS, Baldi P, Sassone-Corsi P. Coordination of the transcriptome and metabolome by the circadian clock. Proc Natl Acad Sci USA. 2012; 109: 5541-5546.

36. Tahara Y, Yamazaki MY, Sukigara H, Motohashi H, Sasaki H, Miyakawa H, Haraguchi A, Ikeda Y, Fukuda S, Shibata S. Gut microbiota-derived short chain fatty acids induce circadian clock entrainment in mouse peripheral tissue. Sci Rep. 2018; 8: 1395.

37. Agus A, Planchais J, Sokol H. Gut microbiota regulation of tryptophan metabolism in health and disease. Cell Host Microbe. 2018; 23: 716-724.

38. Tsukahara T, Matsuda Y, Haniu H. Lysophospholipid-related diseases and PPARγ signaling pathway. Int J Mol Sci. 2017; 18: 2730.

39. Wiedeman AM. Dietary choline intake: current state of knowledge across the life cycle. Nutrients. 2018; 10: 1513.

40. Guo TT, Song D, Cheng L, Zhang X. Interactions of tea catechins with intestinal microbiota and their implication for human health. Food Sci Biotechnol. 2019; 28(6): 1617-1625.

41. Ide K, Matsuoka N, Yamada H, Furushima D, Kawakami K. Effects of tea catechins on Alzheimer's disease: recent updates and perspectives. Molecules. 2018; 23: 2357.

42. Zhang XJ, Choi FFK, Zhou Y, Leung FP, Tan S, Lin SH, Xu HX, Jia W, Sung JJY, Cai ZW, et al. Metabolite profiling of plasma and urine from rats with TNBS-induced acute colitis using UPLC-ESI-QTOF-MS-based metabonomics–a pilot study. FEBS J. 2012; 279: 2322-2338.

43. Deters BJ, Saleem M. The role of glutamine in supporting gut health and neuropsychiatric factors. Food Sci Hum Well, 2021; 10: 149-154.

44. de Souza AZZ, Zambom AZ, Abboud KY, Reis SK, Tannihão F, Guadagnini D, Saad MJA, Prada PO. Oral supplementation with L-glutamine alters gut microbiota of obese and overweight adults: a pilot study. Nutrition. 2015;31: 884-889.

45. Zhu YH, Huan F, Wang JF, Xie XX, Yu GQ, Wang X, Jiang L, Gao R, Xiao H, Ding HX, et al. 1-Methyl-4-phenyl-1,2,3,6-tetrahydropyridine induced Parkinson's disease in mouse: potential association between neurotransmitter disturbance and gut microbiota dysbiosis. ACS Chem Neurosci. 2020; 11: 3366-3376.

46. Gray LR, Tompkins SC, Taylor EB. Regulation of pyruvate metabolism and human disease. Cell Mol Life Sci. 2014; 71: 2577-604.

47. Mukherji A, Bailey SM, Staels B, Baumert TF. The circadian clock and liver function in health and disease. J Hepatol. 2019; 71: 200-211.

48. Matenchuk BA, Mandhane PJ, Kozyrskyj AL. Sleep, circadian rhythm, and gut microbiota. Sleep Med Rev. 2020; 53: 101340.

49. Videnovic A, Lazar AS, Barker RA, Overeem S. 'The clocks that time us'–circadian rhythms in neurodegenerative disorders. Nat Rev Neurol. 2014; 10: 683-693.

50. Musiek ES, Lim MM, Yang GR, Bauer AQ, Qi L, Lee Y, Roh JH, Ortiz-Gonzalez X, Dearborn JT, Culver JP, et al. Circadian clock proteins regulate neuronal redox homeostasis and neurodegeneration. J Clin Invest. 2013; 123: 5389-5400.

51. Agus A, Planchais J, Sokol H. Gut microbiota regulation of tryptophan metabolism in health and disease. Cell Host Microbe. 2018; 23(6): 716-724.

52. Han XN, Chen M, Wang FS, Windrem M, Wang S, Shanz S, Xu QW, Oberheim NA, Bekar L, Betstadt S,et al. Forebrain engraftment by human glial progenitor cells enhances synaptic plasticity and learning in adult mice. Cell Stem Cell. 2013; 12: 342-53.

53. Wasling P, Daborg J, Riebe I, Andersson M, Portelius E, Blennow K, Hanse E, Zetterberg H. Synaptic retrogenesis and amyloid-beta in Alzheimer's disease. J Alzheimers Dis. 2009; 16: 1-14.

54. Guo TT, Song D, Ho C-T, Zhang X, Zhang CD, Cao JX, Wu ZF. Omics analyses of gut microbiota in a circadian rhythm disorder mouse model fed with oolong tea polyphenols. J Agric Food Chem. 2019; 67: 8847-8854.

55. Barbieri R, Coppo E, Marchese A, Daglia M, Sobarzo-Sánchez E, Nabavi SF, Nabavi SM. Phytochemicals for human disease: an update on plant-derived compounds antibacterial activity. Microbiol Res. 2017; 196: 44-68.

56. Cheng M, Zhang X, Zhu JY, Cheng L, Cao JX, Wu ZF, Weng PF, Zheng XJ. Metagenomics analysis of gut microbiota modulatory effect of green tea polyphenols by high fat diet-induced obesity mice model. J Func Foods. 2018; 46: 268-277.

57. Choi BSY, Daniel N, Houde VP, Ouellette A, Marcotte B, Varin TV, Vors C, Feutry P, Ilkayeva O, Ståhlman M, et al. Feeding diversified protein sources exacerbates hepatic insulin resistance via increased gut microbial branched-chain fatty acids and mTORC1 signaling in obese mice. Nat Commun. 2021; 12: 3377.

58. Hamood HM, Al-Zubaidy AA. Neuroprotective effects of vitex agnus castus extract in rats' model of Alzheimer's disease. Eurasia. J Biosci. 2020; 14: 4165-4169.

59. Ren B, Wang LF, Shi L, Jin X, Liu Y, Liu RH, Yin F, Cadenas E, Dai XS, Liu ZG, et al. Methionine restriction alleviates age-associated cognitive decline via fibroblast growth factor 21. Redox Biol. 2021; 41: 101940.

60. Bolyen E. Reproducible, interactive, scalable and extensible microbiome data science using QIIME 2. Nat Biotechnol, 2019; 37: 852-857.

61. Koohi-Moghadam M, Borad MJ, Tran NL, Swanson KR, Boardman LA, Sun HZ, Wang JW. MetaMarker: a pipeline for de novo discovery of novel metagenomic biomarkers. Bioinformatics. 2019; 35: 3812-3814.

62. Qiu YX, Yu HH, Hu Yi, Guo SY, Lei XN, Qin Y, Jian YQ, Li B, Liu LP, Peng CY. Transcriptomic and metabonomic profiling reveal the anti-obesity effects of Chikusetsusaponin V, a compound extracted from Panax japonicus. J Pharm. Pharmacol.2021; 73: 60-69.

63. Want EJ, Wilson ID, Gika H, Theodoridis G, Plumb RS, Shockcor J, Holmes E, Nicholson JK. Global metabolic profiling procedures for urine using UPLC-MS. Nat Protoc. 2010; 5: 1005-1018.

64. Yuan M, Breitkopf SB, Yang X, Asara JM. A positive/negative ion-switching, targeted mass spectrometry-based metabolomics platform for bodily fluids, cells, and fresh and fixed tissue. Nat Protoc. 2012; 7: 872-881.

65. Zhu XS, Li HD, Guo LL, Wu FX, Wang JX. Analysis of single-cell RNA-seq data by clustering approaches. Curr Bioinform. 2019; 14: 314-322.

66. Kramer A, Green J, Pollard J, Tugendreich S. Causal analysis approaches in ingenuity pathway analysis. Bioinformatics. 2014; 30: 523-530.

67. Bindea G, Mlecnik B, Hackl H, Charoentong P, Tosolini M, Kirilovsky A, Fridman W-H, Pagès F, Trajanoski Z, Galon J. ClueGO: a Cytoscape plug-in to decipher functionally grouped gene ontology and pathway annotation networks. Bioinformatics. 2009; 25: 1091-1093.

Figures

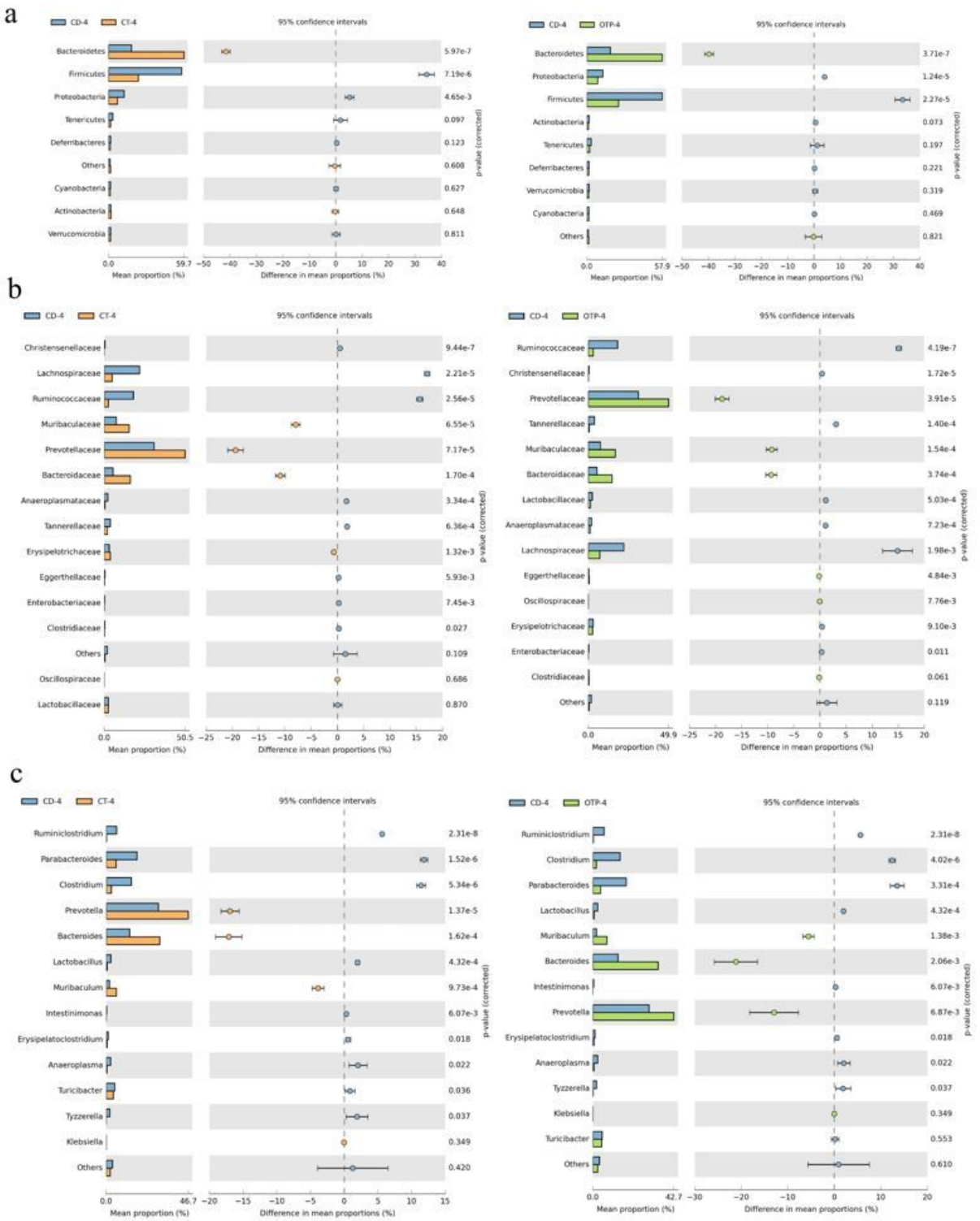

Figure 1

The relative abundance of intestinal flora at the phylum (a), families (b) and genus (c) from samples (the relative abundance of intestinal flora of each input sample was analyzed using STAMP).

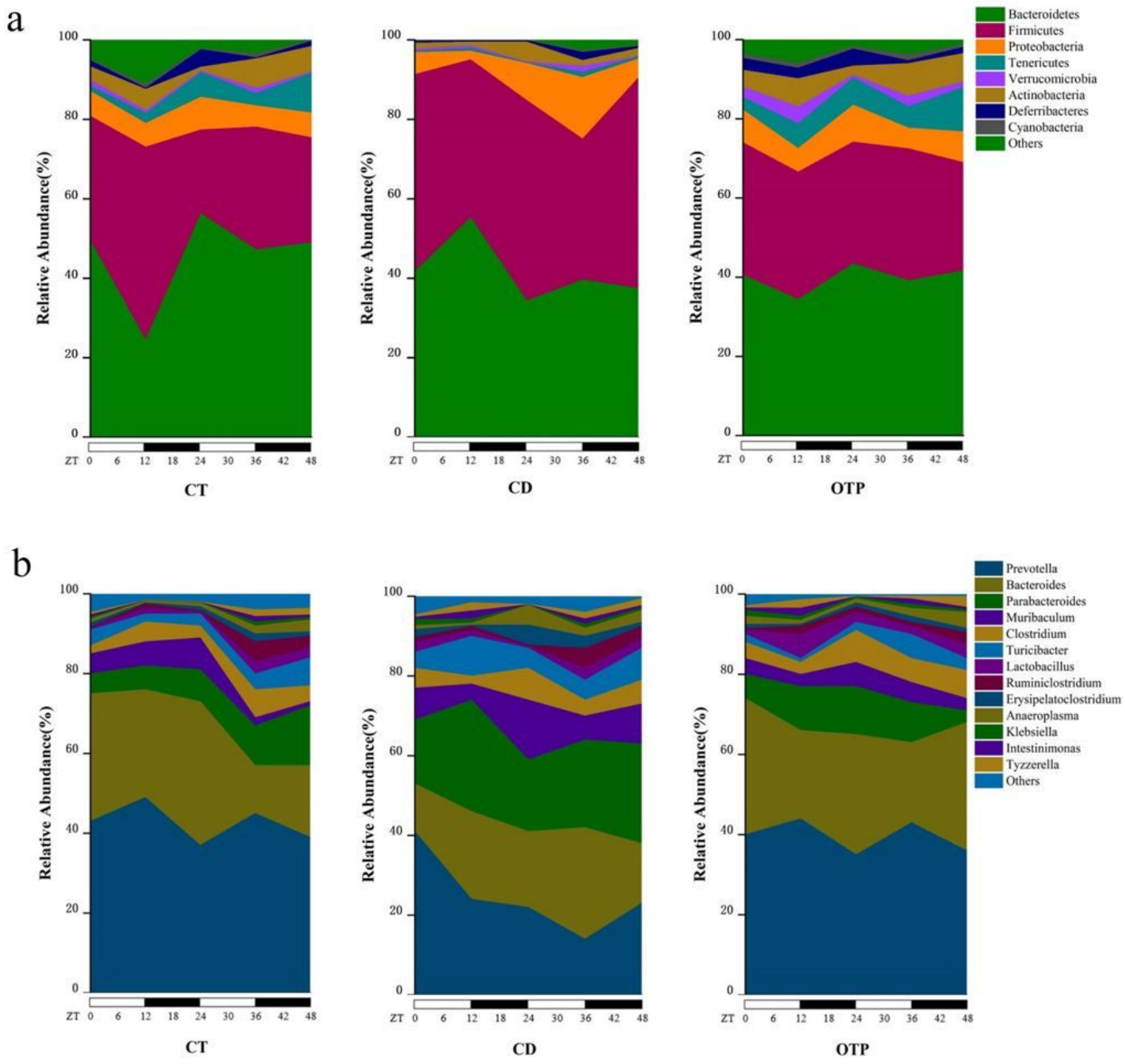

Figure 2

The variation in the diurnal oscillations of the representative bacteria at the phylum level (a) and the genus level (b).

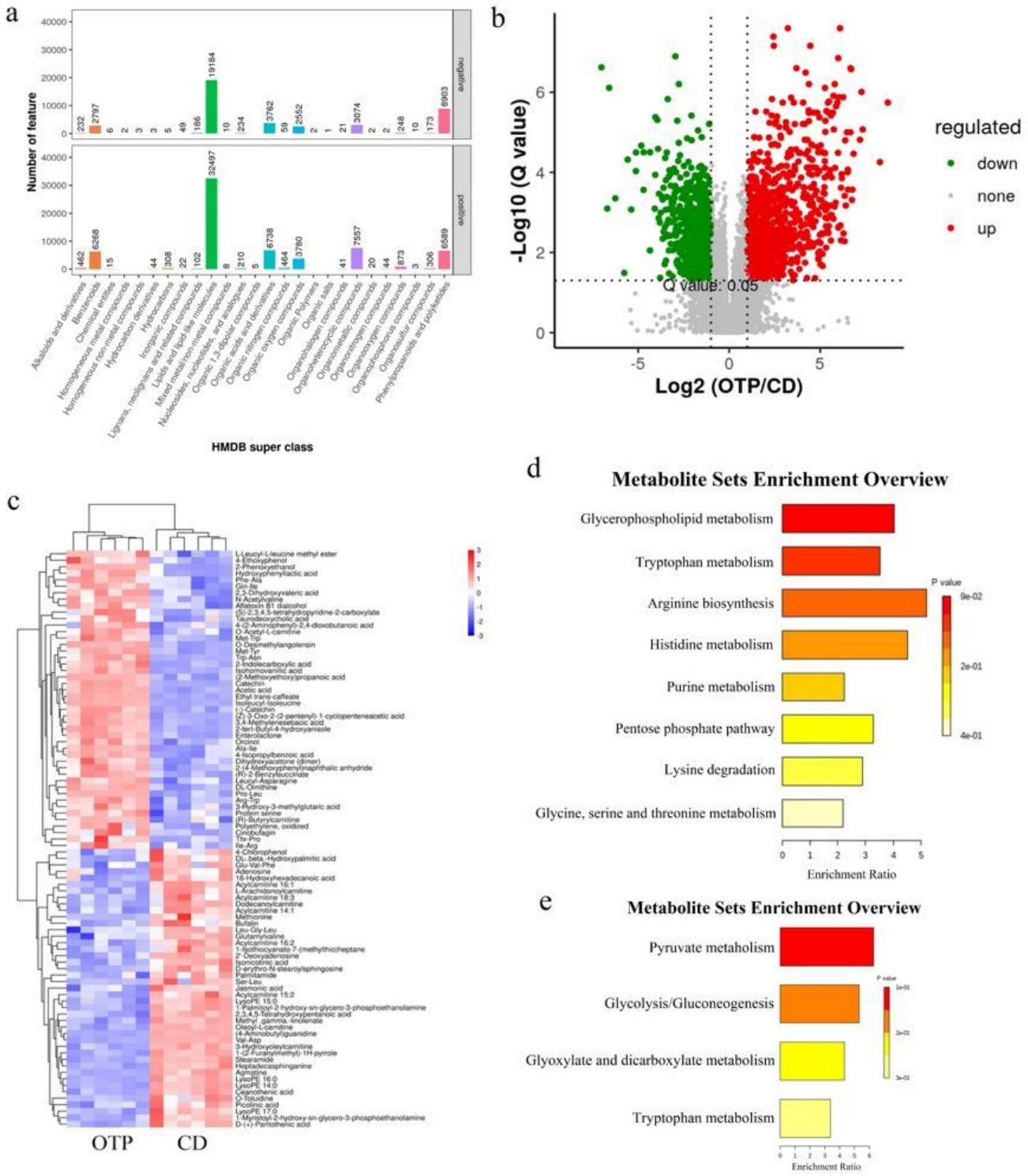

Figure 3

Effects of OTP on metabolomic changes in circadian rhythm disorder mice model. a. HMDB super class identification classification and annotation diagram of first-level metabolites; b. volcano plots of the different metabolites in the OTP and CD groups; c. heat map of significantly differential metabolites between the CD group and OTP group; d. KEGG (KEGG: Kyoto Encyclopedia of Genes and Genomes) enrichment pathways of significantly down-regulated differential metabolites between the CD group and

CT group; e. KEGG enrichment pathways of significantly up-regulated differential metabolites between the CD group and OTP group. * p < 0.05, **p < 0.01.

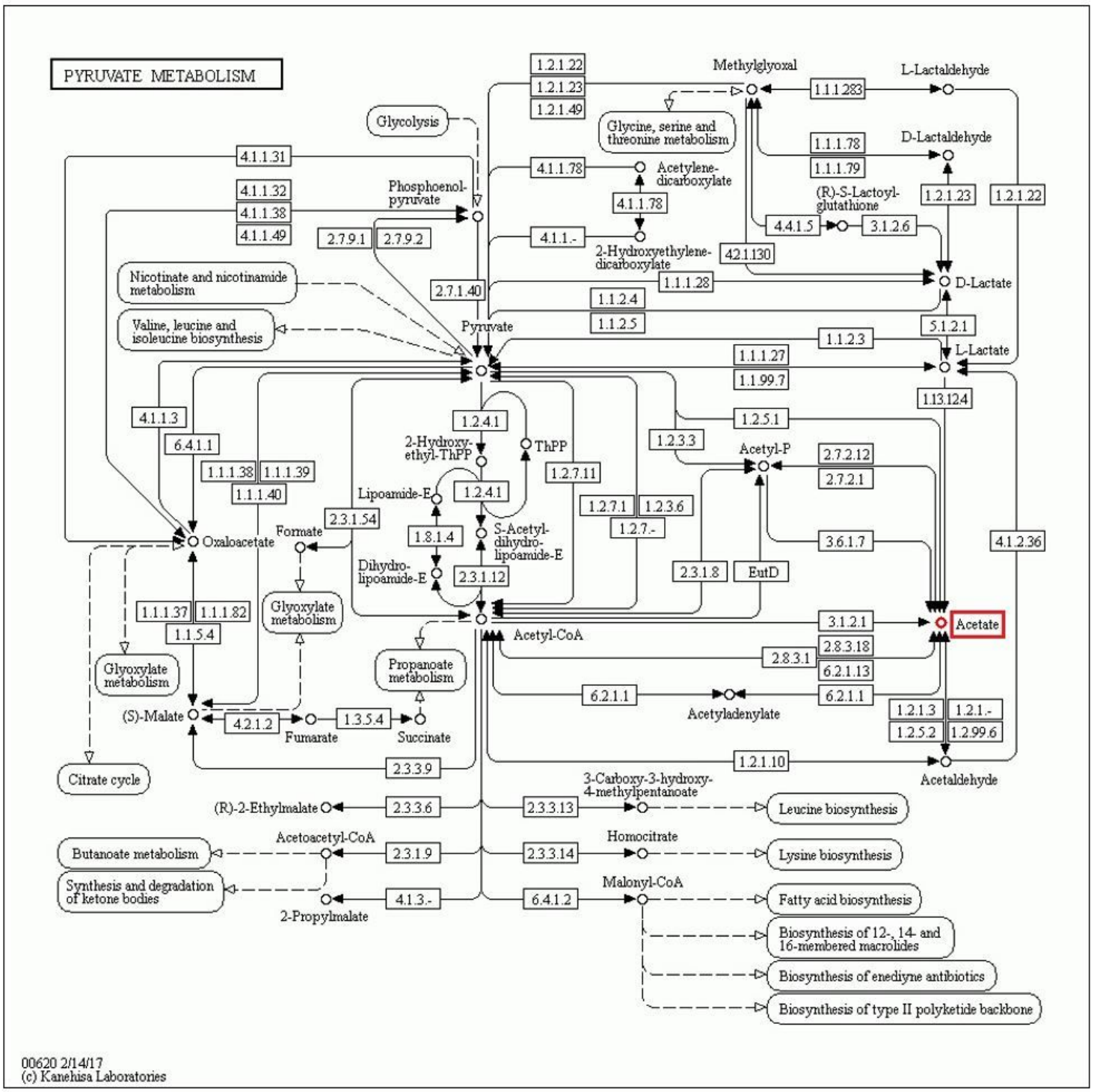

Figure 4

Overview of the pyruvate metabolism after the intervention of OTP in KEGG. Red indicated the metabolite content was up-regulated.

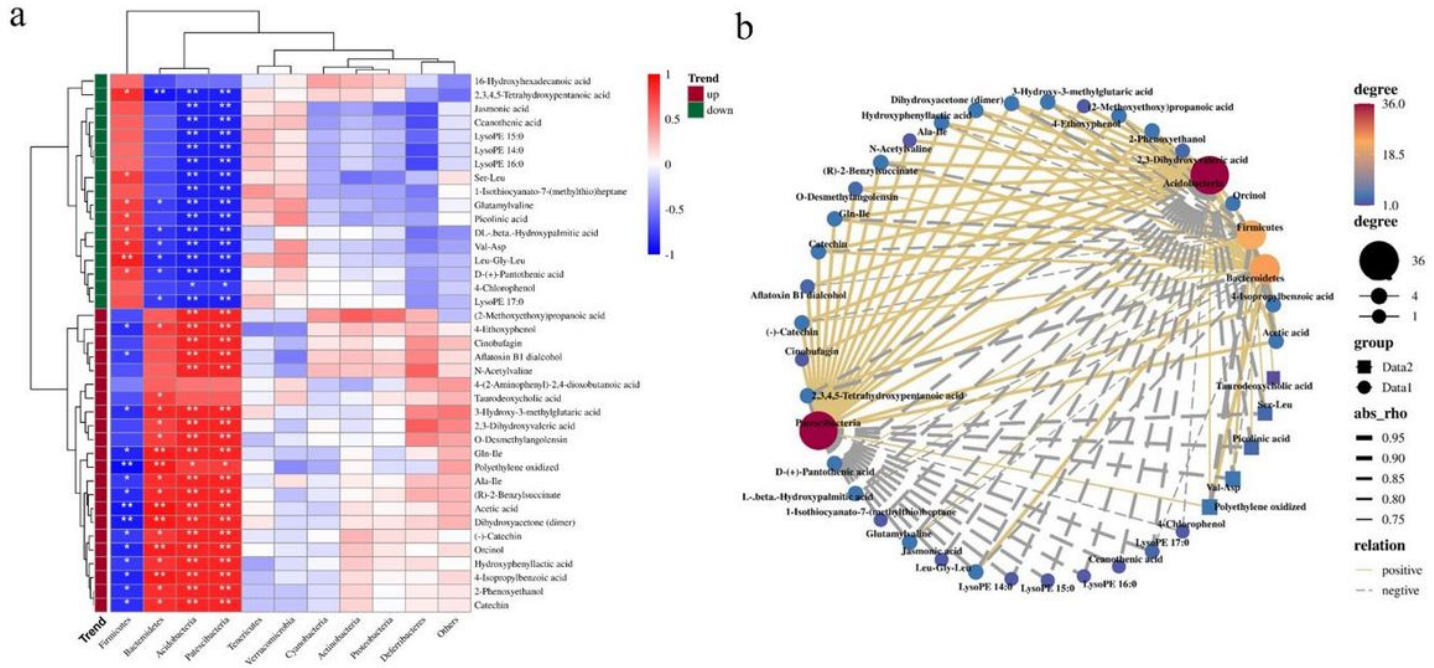

Figure 5

The correlation between intestinal microbiota and intestinal differential metabolites. a. correlation heat map between intestinal differential metabolites and microbiota in CD and OTP groups in NIM; b. network diagram of intestinal differential metabolites and microbiota. * $p < 0.05$, **$p < 0.01$.

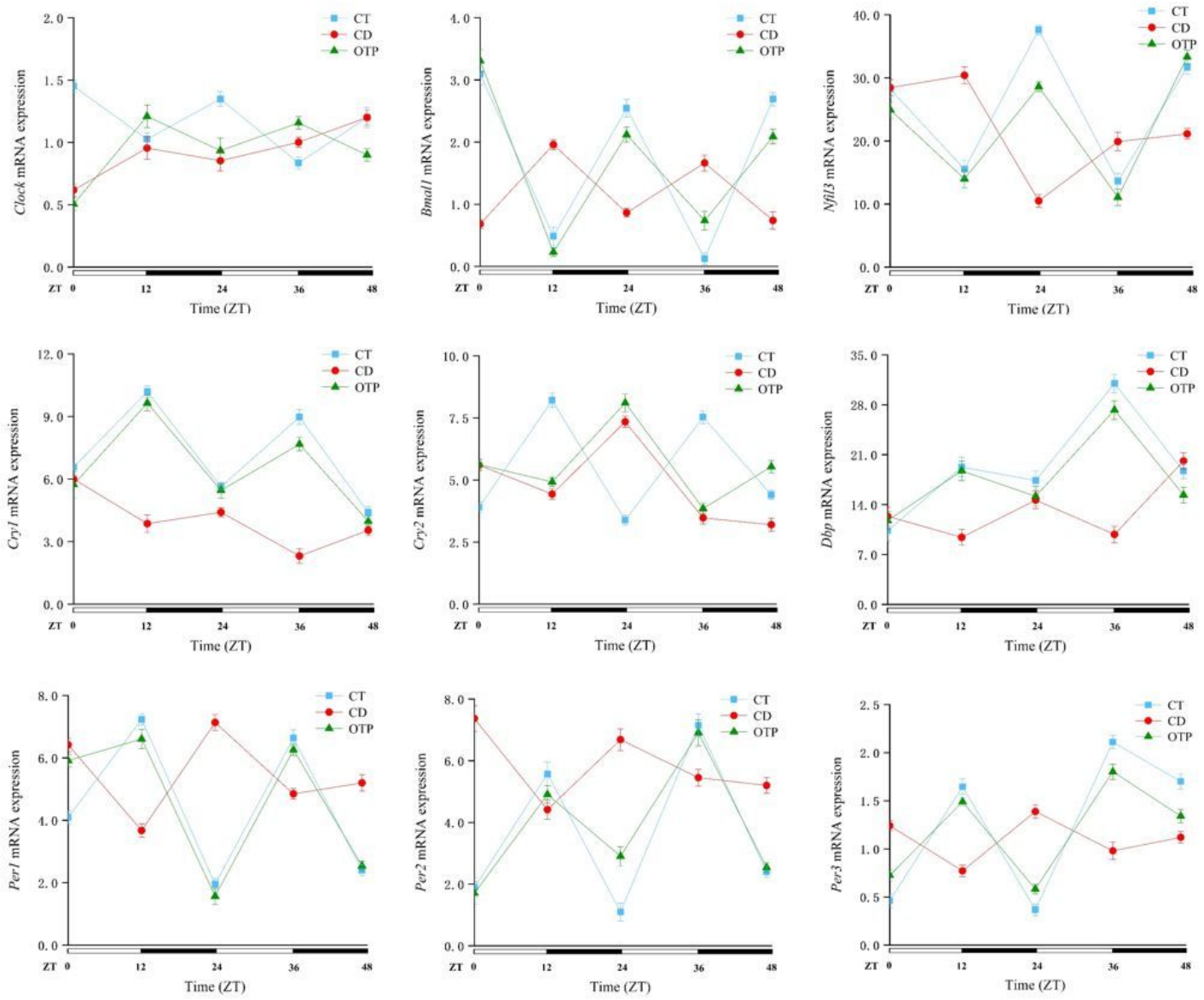

Figure 6

The mRNA levels of Clock, Bmal1, Cry1, Cry2, Per1 and other liver clock genes at different time points of the day.

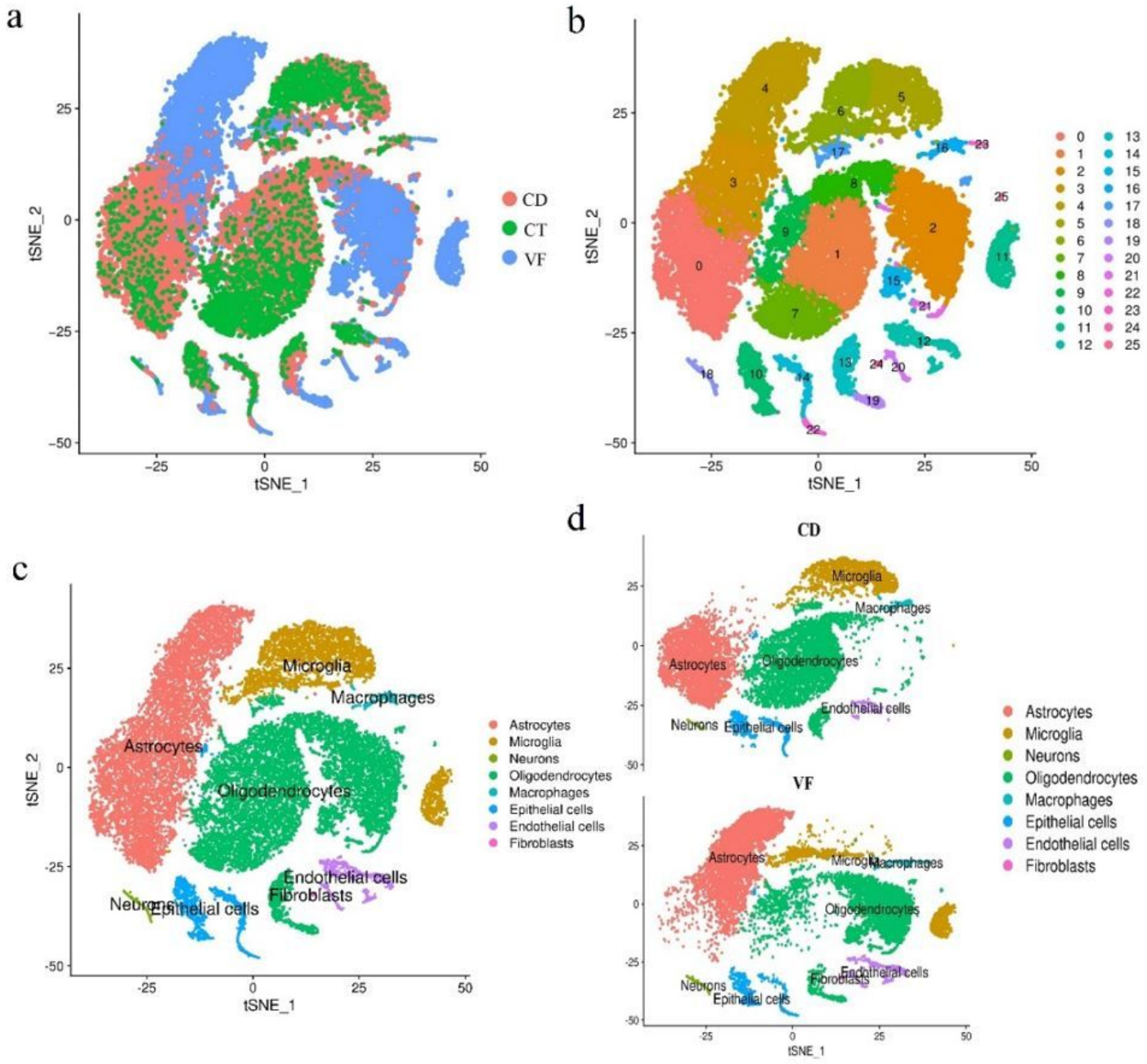

Figure 7

Effects of OTP on hypothalamic cell types in mice with rhythm disturbance. a. t-SNE map of single cells of hypothalamus in CD, CT and VF groups; b. t-SNE images of total hypothalamic cells in different clusters; c. t-SNE identification map of hypothalamic single-cell in the CT, CD and VF group of samples; d. distribution of cells from the CD group and VF group across all cell types.

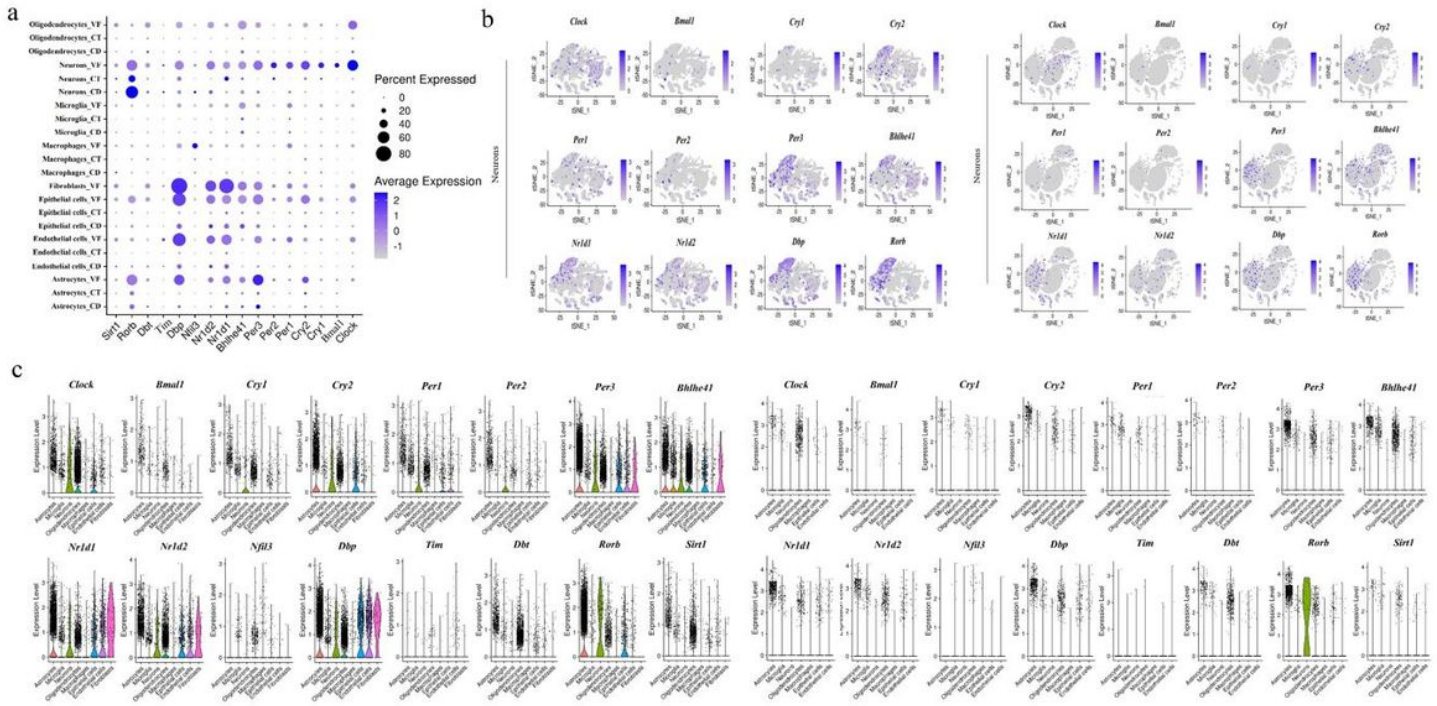

Figure 8

Effects of OTP on hypothalamic genes in mice with rhythm disturbance. a. dot plots of circadian rhythm genes expression level of specific cell in the three groups; b. t-SNE map of the expression of rhythm genes in neurons in the VF group (left) and CD group (right); c. violin plot of the expression of circadian rhythm genes in VF group (left) and CD group (right) of the mainly cell types.

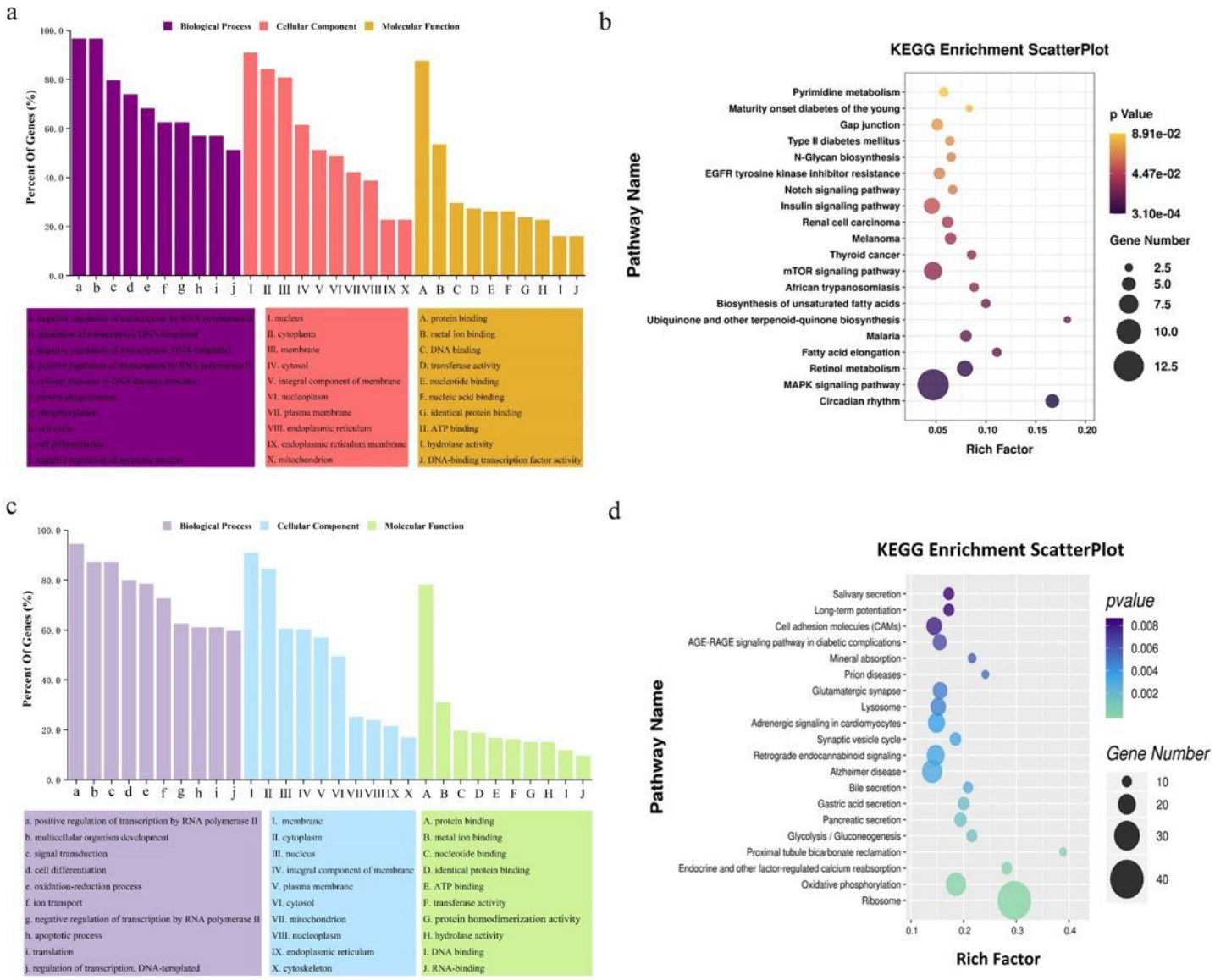

Figure 9

Effects of OTP intervention on gene enrichment pathway in liver and hypothalamus. (a) GO classification analysis in liver between the CD group and OTP group; (b) KEGG pathway analysis in liver between the CD group and OTP group; (c) GO classification analysis in hypothalamus between the CD group and VF group; (d) KEGG pathway analysis in liver between the CD group and VF group.

Supplementary Files

This is a list of supplementary files associated with this preprint. Click to download.

- AbstractFigure.jpg
- FigureS1.jpg
- FigureS2.jpg

- FigureS3.jpg
- FigureS4.jpg
- FigureS5.jpg
- FigureS6.jpg
- FigureS7.jpg
- FigureS8.jpg
- FigureS9.jpg
- TableS1.xlsx
- TableS2.xlsx
- TableS3.xlsx